Robustness of persistent spiking to partial synchronization in a minimal model of synaptically driven self-sustained activity

Nikita Novikov[1] and Boris Gutkin[1,2]

[1]*Centre for Cognition and Decision Making, National Research University Higher School of Economics, Moscow 101000, Russia*

[2]*Group for Neural Theory, LNC INSERM U960, Department of Cognitive Studies, Ecole Normale Superieure PSL* Research University, Paris 75005, France*

(Received 20 July 2016; revised manuscript received 7 October 2016; published 21 November 2016)

We study the behavior of a minimal model of synaptically sustained persistent activity that consists of two quadratic integrate-and-fire neurons mutually coupled via excitatory synapses. Importantly, each of the neurons is excitable, as opposed to an oscillator; hence when uncoupled it sits at a subthreshold rest state. When the constituent neurons are mutually coupled via sufficiently strong fast excitatory synapses, the system demonstrates bistability between a fixed point (quiescent background state) and a limit cycle (memory state with synaptically driven spiking activity). Previous work showed that this persistent activity can be stopped by an excitatory input that synchronizes the network. Here we analyzed how this persistent state reacts to partial synchronization. We considered three types of progressively more complex excitatory synaptic kernels: delta pulse, square, and exponential. The first two cases were treated analytically, and the latter case numerically. Using phase-plane methods, we characterized the shape of the region, such that all orbits starting within it correspond to infinite spike trains; this constitutes the persistent activity region. In the case of instant coupling, all such active orbits were neutrally stable; in the case of noninstant coupling, the activity region contained a unique stable limit cycle (so the activity region was the basin of attraction for the limit cycle). This limit cycle corresponded to purely antiphase spiking of two neurons. Increasing synchronization shifted the system toward the border of the activity region, eventually terminating spiking activity. We calculated three measures of robustness of the active state: width of the activity region in the phase plane, critical level of synchronization that can be tolerated by the persistent spiking activity, and speed of reconvergence to the limit cycle. Our analysis revealed that the self-sustained activity is more robust to synchronization when each individual neuron is closer to SNIC bifurcation (closer to being an intrinsic oscillator), the recurrent synaptic excitation is stronger, and the synaptic decay is slower, which is in agreement with the existing data on local circuits in the cortex that show sustained activity.

DOI: 10.1103/PhysRevE.94.052313

I. INTRODUCTION

Working memory, allowing the execution of specific responses that rely on recently remembered information, plays a central role in enabling cognitive abilities. In order to execute working memory based tasks, the information relevant for the response must be held online actively so that it can be used rapidly and efficiently. The prevalent neural mechanism for working memory is persistent spiking activity in neural circuits [1–3]. Persistent activity is evoked by presentation of transient stimuli (relevant to the task), that can be modeled as brief input pulses to the neural circuit. This activity lasts for a prolonged time period (up to seconds), and it is believed to underlie various brain functions that go beyond working memory—from gaze stabilization to memory-dependent attentional modulation and executive control [4]. The ability of a circuit to generate different levels of activity in the presence of the same time-invariant input and to switch between them after transient input pulses corresponds to multistability in the mathematical model that describes the circuit. One of the key mechanisms proposed for generation of such multistable behavior is self-sustained synaptic reverberation of excitation in neural networks with the appropriate level of interconnectivity [5]. In the simplest case, a system is bistable: The first stable manifold corresponds to the background regime with low firing rates, and the second one corresponds to the active maintenance of information by the network reflected in self-sustained spiking activity with elevated firing rates. In deterministic spiking neural circuits, the generic picture is that the constituent neurons are excitable (i.e., they do not fire without sufficient synaptic input) and the self-sustained activity is produced by synaptic interactions and corresponds to a limit cycle or a collection of limit cycles. Interestingly, proximity of the orbit to the limit cycle is related to the temporal structure of firing. It has been shown that the self-sustained activity should be almost asynchronous: splay state for large networks [6] where for any two successive spikes of a given neuron in the network, the spikes of the other neurons are maximally "splayed out" equally in time. In other words, there is no clustering of spike times. For a minimal two-neuron model this corresponds to an antiphase "ping-pong" firing [7,8]. Furthermore, it has been noted that strong enough partial synchronization can move the system out of the active regime thus terminating self-sustained activity [6,7,9]. Recently we proposed that control over synaptically sustained activity in large circuits can be implemented by either changes in input correlations and/or frequency shifts in global input oscillations, again pointing toward input-modulated synchrony within the sustained activity pattern. However, the precise mechanisms by which even partial synchronization may terminate self-sustained activity have not been fully characterized. This motivates the present study of the basin of attraction structure for a minimal model of a steady-state–limit-cycle bistable system, as well as a characterization of the critical partial synchrony level required for pushing the system out of the basin of attraction that exists around the limit cycle.

To determine the specific conditions on the transient partial synchrony and robustness of sustained firing we turned to a minimal model that is able to demonstrate the type of bistability described above: background rest state and a sustained firing regime, as well as relative asynchrony of the activity. This minimal model should also consist of neural equations that reflect the active spike generation and be simple enough to be amenable to analysis (e.g., by phase- plane methods since our previous work allowed us to conjecture that the geometry of the region for the active regime matters). We thus focused on a minimal model that consists of two excitable type I neurons (either receiving tonic inhibition from an external source or having the stable subthreshold state and a threshold due to passive membrane currents) mutually coupled by fast excitatory synapses that are sufficiently strong [7]. For the single-cell equations we picked the quadratic integrate-and-fire neuron (QIF). The QIF is the canonical one-dimensional model for type I excitable neurons and is directly related to the normal form for the saddle node on an invariant circle bifurcation that underlies type I excitability [10,11]. The QIF, when interpreted in terms of voltage, includes the active spike generation reflected in the solutions that trend to infinity in finite time if the state variable pushed above the saddle threshold. This explosion to infinity models the active spike generation. Practically speaking, the voltage in the QIF can be reset at a sufficiently large finite value without loss of generality [12]. The QIF and the related theta neuron have been previously used in multiple studies of neuronal dynamics [12,13] and models of working memory [14]. The coupling between the neurons is modeled by voltage-dependent synapses that reflect AMPA recurrent.

This minimal model shows important dynamical hallmarks of the sustained firing observed in larger models of working memory [14,15] and hinted at in experiments in animals performing delayed response tasks [1–3]. Within the minimal model, in the background state, both neurons are quiescent, while in the active regime they alternatively force each other to cross the spiking threshold (by the recurrent synapses) and, consequently, to fire spikes. The behavior of such system is determined by relative timing of spikes: The active state corresponds to antiphase firing, and should it be somehow pushed to be sufficiently strongly synchronized, the system falls to the background state. It should be noted that systems of coupled type I oscillators are studied very well [16], while analytical studies of systems of coupled type I neurons in the excitable regime are less common. For a large network of recurrently coupled excitable type I neurons, it was shown that the splay state (analogous to the antiphase state of the two-neuron system) is stable when synaptic coupling between neurons is noninstant [8].

In the present study, we expand on work by Gutkin *et al.* [6], and analyze a system of two synaptically coupled excitatory quadratic integrate-and-fire neurons with the input currents being negative in the absence of synaptic activity. The main goal of our analysis is to systematically investigate how robustness of the sustained activity to partial synchronization depends on parameters of the model circuit. We use the term "robustness" in the nonstrict sense, assuming that the sustained activity is more robust if stronger synchronizing perturbation of the system's state should be applied to terminate it and if the system returns faster to the asynchronous regime after a perturbation that did not terminate the activity. Instead of explicitly perturbing the state, we analyze the phase space of the system and derive three measures of robustness: (1) width of the region of self-sustained activity on the phase plane, (2) speed of convergence to the limit cycle (if the system has one), and (3) critical level of synchronization between spikes of two neurons that leads to termination of the activity.

This paper is organized as follows. First, we describe our model and introduce main definitions and equations. We lay out the background by drawing the structure of the solution flows, fixed points, and associated solutions (e.g., the stable and unstable heteroclinics for the saddle points) for two uncoupled neurons. We then build on that to draw the structure of the phase space for the coupled system including the region of self-sustained spiking activity. The geometry of this region, that is also the basin of attraction for the stable limit cycle in the case of noninstant coupling, gives us qualitative hints about how robust the activity is to various perturbations. We shore up the qualitative analysis by computing the curve of maximal synchronization that does *not* move the system out of the active region or, in other words, does *not* terminate persistent activity. We present the structure of the activity region and the maximal synchronization curves obtained for the systems with different types of coupling: (1) uncoupled system, (2) system with instant interaction, (3) system with square synaptic kernel, and (4) system with exponential synaptic kernel. We then look at how robustness depends on key parameters of the model: intrinsic cell properties, synaptic strengths, and time scales. We demonstrate that the self-sustained antiphase firing mode is stable in the case of noninstant synaptic coupling, and that it is more robust when each of the constituent neurons is closer to its intrinsic bifurcation and synaptic coupling is stronger and slower. Finally, we summarize our results in a context of previous results.

II. METHODS

In the present paper, we analyze a system of two excitable quadratic integrate-and-fire (QIF) neurons coupled by excitatory synapses. First, we introduce notation related to dynamics of a single QIF neuron and describe equations that govern these dynamics. Next, we do the same for the system of two coupled neurons. Specifically, we describe synaptic kernels analyzed in this paper, and discuss an approach to making the synaptically coupled system autonomous by moving from time-dependent to voltage-dependent synaptic kernels. We also introduce notations for spike-to-spike mapping of the system state. Finally, we define the measures of robustness that we use in this manuscript and relate them to generally accepted notions of stability.

A. Quadratic integrate-and-fire neuron

We start by describing a solution for voltage dynamics of a single QIF neuron receiving constant input current:

$$\frac{dx}{dt} = x^2 + I, \quad x \leftarrow -\infty \text{ if } x = \infty. \tag{1}$$

The neuron is considered to fire a spike when its voltage diverges to infinity.

Assuming that the voltage of a neuron at zero time moment was x_0, we will use the following notation for the voltage at the time t:

$$x(t) = \phi_I(x_0,t). \tag{2}$$

We will also use the following notation for the time during which the voltage changes from x_0 to x:

$$t = T_I(x_0,x). \tag{3}$$

Let us denote $\hat{a} = \sqrt{|I|}$. The expressions for ϕ_I and T_I depend on the sign of I, which leads to the following three cases.

(a) The neuron is excitable if $I < 0$:

$$x(t) = \phi_I^{\text{ex}}(x_0,t) = -b_{\text{ex}} + \frac{{b_{\text{ex}}}^2 - \hat{a}^2}{b_{\text{ex}} - x_0},$$
$$b_{\text{ex}} = \frac{\hat{a}}{\tanh(\hat{a}t)}. \tag{4}$$
$$t = T_I^{\text{ex}}(x_0,x) = \frac{1}{\hat{a}}\operatorname{arctanh}\frac{\hat{a}(x-x_0)}{x_0x - \hat{a}^2},$$
$$x_0 \leqslant x \leqslant -a \quad \text{or} \quad -a \leqslant x \leqslant x_0 \leqslant a \quad \text{or} \quad a \leqslant x_0 \leqslant x. \tag{5}$$

(b) The neuron is oscillatory if $I > 0$:

$$x(t) = \phi_I^{\text{osc}}(x_0,t) = -b_{\text{osc}} + \frac{{b_{\text{osc}}}^2 + \hat{a}^2}{b_{\text{osc}} - x_0},$$
$$b_{\text{osc}} = \frac{\hat{a}}{\tan(\hat{a}t)}. \tag{6}$$
$$t = T_I^{\text{osc}}(x_0,x) = \begin{bmatrix} \frac{1}{\hat{a}}\arctan\frac{\hat{a}(x-x_0)}{x_0x+\hat{a}^2}, & x_0x + \hat{a}^2 \geqslant 0 \\ \frac{\pi}{\hat{a}} + \frac{1}{\hat{a}}\arctan\frac{\hat{a}(x-x_0)}{x_0x+\hat{a}^2}, & x_0x + \hat{a}^2 < 0 \end{bmatrix},$$
$$x_0 \leqslant x. \tag{7}$$

(c) The neuron is at its bifurcation (saddle node on an invariant circle) $I = 0$:

$$x(t) = \phi_I^{\text{bif}}(x_0,t) \equiv -b_{\text{bif}} + \frac{{b_{\text{osc}}}^2}{b_{\text{bif}} - x_0}, \quad b_{\text{osc}} = \frac{1}{t}, \tag{8}$$
$$t = T_I^{\text{bif}}(x_0,x) = \frac{x - x_0}{x_0x},$$
$$x_0 \leqslant x \leqslant 0 \quad \text{or} \quad x_0 \leqslant x \leqslant 0. \tag{9}$$

The case (c) is degenerate, so we will concentrate on the cases (a) and (b).

Using (5) and (7), we can express time $\tilde{T}_I$ since the last spike that is needed for a neuron to reach voltage x:

$$\tilde{T}_I^{\text{ex}}(x) = \begin{bmatrix} -\frac{1}{\hat{a}}\operatorname{arctanh}\frac{\hat{a}}{x}, & x \leqslant -a \\ \infty, & x > -a \end{bmatrix}. \tag{10}$$

$$\tilde{T}_I^{\text{osc}}(x) = \begin{bmatrix} -\frac{1}{\hat{a}}\arctan\frac{\hat{a}}{x}, & x \leqslant 0, \\ \frac{\pi}{\hat{a}} - \frac{1}{\hat{a}}\arctan\frac{\hat{a}}{x}, & x > 0 \end{bmatrix}. \tag{11}$$

B. Two-neuron model description

Now let us consider a system of two coupled quadratic integrate-and-fire (QIF) neurons (denoted by X and Y):

$$\begin{aligned} \frac{dx}{dt} &= x^2 + I_{\text{ext}} + I_{\text{syn}}^x, \\ \frac{dy}{dt} &= y^2 + I_{\text{ext}} + I_{\text{syn}}^y, \\ x &\leftarrow -\infty \ \text{ if } \ x = \infty, \\ y &\leftarrow -\infty \ \text{ if } \ y = \infty, \end{aligned} \tag{12}$$

where x, y are voltages of neurons X and Y respectively; $I_{\text{ext}} < 0$ is the constant inhibitory current; I_{syn}^x, I_{syn}^y are the input synaptic currents of neurons X and Y, respectively. Neuron X (Y) is considered to produce a spike when $x = \infty$ ($y = \infty$).

To simplify the equations, we will use the notation

$$a = \sqrt{|I_{\text{ext}}|}. \tag{13}$$

Note that a in (13) is related to the tonic input current only, while $\hat{a}$ in (4)–(11) is related to the total input current. We also use the following notation for phases of neurons X and Y:

$$\begin{aligned} \theta_x &= 2\arctan x, \\ \theta_y &= 2\arctan y. \end{aligned} \tag{14}$$

When voltage x goes to infinity and resets to minus infinity, phase θ_x passes through the value $\theta_x = \pi$; the same is true for y and θ_y. The QIF model rewritten using the phase notations is known as the theta model [11].

The synaptic current received by neuron X at the time t depends, in general, on the time passed since the last spike of neuron Y (and vice versa):

$$\begin{aligned} I_{\text{syn}}^x(t) &= K(t - t_y), \\ I_{\text{syn}}^y(t) &= K(t - t_x), \end{aligned} \tag{15}$$

where t_x and t_y are the times of the last spikes of neurons X and Y, respectively (if a neuron produced no spikes in the past, the corresponding time can be considered as $-\infty$), and $K(\Delta t)$ is a synaptic kernel function depending on the time Δt passed since the last spike. In this paper, we consider the following four types of synaptic interactions.

(a) No interaction (uncoupled system):

$$K(\Delta t) = 0. \tag{16}$$

(b) Instant synaptic interaction:

$$K(\Delta t) = J\delta(\Delta t), \tag{17}$$

where J is the synaptic weight, and δ the Dirac delta function. In this case, when a neuron fires a spike, voltage of another neuron instantaneously increases by J.

(c) Interaction via synapse with square kernel:

$$K(\Delta t) = Jh(\Delta t)h(\tau_s - \Delta t), \tag{18}$$

where J is the synaptic weight, τ_s the "width" of the synaptic kernel, and $h(\cdot)$ is the Heaviside step function. In this case, a constant synaptic current is received by a neuron during the time τ_s after a spike of another neuron.

(d) Interaction via synapse with exponential kernel:

$$K(\Delta t) = J \exp \frac{-\Delta t}{\tau_s} h(\Delta t), \tag{19}$$

where J is the synaptic weight (amplitude of postsynaptic current step), τ_s the width of the synaptic kernel (time constant of synaptic current decay), and $h(\cdot)$ the Heaviside step function. In this case, synaptic current exponentially decays as the time since the last spike increases.

Let us assume that the synaptic current decays sufficiently fast compared to the interval between adjacent spikes of two neurons. In this case, at the time moment t_x when neuron X fires a spike, the input synaptic current $I^x_{\text{syn}}(t_x)$ (initiated by a previous spike of neuron Y) is negligible and can be considered to be zero. We can also consider that $I^x_{\text{syn}}(t) = 0$ for any t from the time interval between t_x and the moment of firing the next spike by neuron Y. Consequently, the voltage $x(t)$ is not affected by the history of the system that preceded t_x, so $x(t)$ and $t - t_x$ are in one-to-one correspondence given by (4) and (10):

$$\begin{aligned} x(t) &= \phi^{\text{ex}}_{I_{\text{ext}}}(-\infty, t - t_x), \\ t - t_x &= \tilde{T}^{\text{ex}}_{I_{\text{ext}}}(x). \end{aligned} \tag{20}$$

The same reasoning applied for neuron Y yields

$$\begin{aligned} y(t) &= \phi^{\text{ex}}_{I_{\text{ext}}}(-\infty, t - t_y), \\ t - t_y &= \tilde{T}^{\text{ex}}_{I_{\text{ext}}}(y), \end{aligned} \tag{21}$$

where t lies between t_y and the time of the following spike of neuron X.

The assumption mentioned above allows us to move from the time-dependent kernels $K(\cdot)$ given by (16)–(19) to the kernels $\tilde{K}(\cdot)$ that depend on the voltage of the recently fired neuron:

$$\begin{aligned} I^x_{\text{syn}}(x,y) &= \tilde{K}(y) \equiv K\left(\tilde{T}^{\text{ex}}_{I_{\text{ext}}}(y)\right), \\ I^y_{\text{syn}}(x,y) &= \tilde{K}(x) \equiv K\left(\tilde{T}^{\text{ex}}_{I_{\text{ext}}}(x)\right). \end{aligned} \tag{22}$$

We should note that using voltage-dependent kernels $\tilde{K}(\cdot)$ instead of time-dependent kernels $K(\cdot)$ has no significant effects on the dynamics of the system only if the synchronization between the neurons is not too strong (i.e., a neuron fires a spike only when its input synaptic current produced by the previous spike of another neuron is already terminated).

Substituting the expressions in (22) into (12) makes the system autonomous, so it can be studied using phase-plane analysis. In order to make the phase portrait more tractable, it is convenient to use the $(\theta_x;\theta_y)$ description instead of the $(x;y)$ description. Obviously, θ_x and θ_y are defined up to 2π, so the phase portrait of the system on the $(\theta_x;\theta_y)$ plane is 2π periodic (or, in other words, it lies on the surface of a torus with the period of 2π). Further in this paper, we will always use (θ_x,θ_y) coordinates for visualizing phase portraits, and (x,y) coordinates for calculations; the legend on phase portraits will be also given in (x,y) coordinates.

C. Useful notation for spike-time maps

Let us denote the state of the system at zero time as (x_0, y_0) and the state of the system at the time t as (x,y). We introduce the following notations:

$$(x,y) = f(x_0, y_0, t), \tag{23}$$

$$t = \tau(x_0, y_0, x, y). \tag{24}$$

Let us assume that neuron Y produces a spike at zero time, and neuron X produces a spike at the time t_x. At the moment of spike firing, voltage of a QIF neuron is infinite, so from (23) and (24) we get

$$(\infty, y) = f(x_0, -\infty, t_x), \tag{25}$$

$$t_x = \tau(x_0, -\infty, \infty, y). \tag{26}$$

We will use the following notation for the mapping from $(x_0, -\infty)$ to (∞, y) and for the corresponding time interval:

$$y = g_1(x_0), \tag{27}$$

$$t_x = \tau_1(x_0). \tag{28}$$

Now let us assume that neuron Y produces the first spike at zero time and the next spike at the time t_y; and that the voltages of neuron X during these two spikes are equal to x_0 and x, respectively. In this case, we will use the notations

$$x = g_2(x_0) = g_1(g_1(x_0)), \tag{29}$$

$$t_y = \tau_2(x_0) = \tau_1(x_0) + \tau_1(g_1(x_0)). \tag{30}$$

In this paper, we refer to $\tau_1(x_0)$ as the time between adjacent spikes (of two neurons), and to $\tau_2(x_0)$ as the interspike interval (i.e., the interval between spikes of the same neuron).

D. Measures of robustness

Further in this paper, we demonstrate that for appropriate parameter combinations there exists an invariant region on the phase plane such that each orbit that starts somewhere in this region remains in this region and so corresponds to an infinite train of spikes (i.e., the system demonstrates self-sustained spiking activity). We refer to it as the activity region. We also show that there exists a special orbit inside the activity region that corresponds to antiphase firing of the two neurons. In the case of noninstant synaptic interaction this orbit is an attracting limit cycle, and in the case of instant interaction it is neutrally stable. In the latter case, we refer to this orbit as the "middle orbit."

We consider the robustness of the system as its ability to stay in the self-sustained spiking mode in the face of state perturbations that push the system from the antiphase orbit toward the borders of the activity region (under constant parameters of the system). In order to mathematically express this invariance, we calculate three robustness measures: (A) width of the activity region D_{act}, (B) speed of convergence to the limit cycle φ_{conv}, and (C) critical shrinking of the interval between the asjacent spikes of the two neurons η_{crit}.

We calculate the width of the activity region along the line on the phase plane that corresponds to firing a spike by one of the neurons. For this purpose, we consider two voltages $x_{\min}$ and $x_{\max}$, such that for each $x_0 \in (x_{\min}, x_{\max})$, the orbit starting from the point $(x_0, -\infty)$ lies inside the activity region, and for any other value of x_0 this condition is not satisfied [e.g., see the bottom part of Fig. 2(a)]. Then we define the width of the activity region as the difference:

$$D_{\text{act}} \equiv x_{\max} - x_{\min}. \tag{31}$$

The wider the activity region is, the more robust the system is, because in this case a stronger state perturbation is needed to push the system outside its borders.

We calculate the speed of convergence to the limit cycle as the inverse of the derivative of spike-to-spike mapping (27) calculated at the point x_m that is the fixed point of this mapping (and thus lies on the limit cycle or middle orbit):

$$\varphi_{\text{conv}} \equiv \left[\left. \frac{dg_1(x_0)}{dx_0} \right|_{x_m} \right]^{-1}. \tag{32}$$

We note that the speed of convergence to the limit cycle is related to the Lyapunov exponent λ by the following expression:

$$e^{\lambda \tau_2(x_m)} = \frac{1}{\varphi^2_{\text{conv}}}, \tag{33}$$

where $\tau_2(x_m)$ is the period of the limit cycle. When φ_{conv} is larger, the system recovers faster after a state perturbation, so the self-sustained activity is more robust if such perturbation is repeated. In the case of instant synaptic interaction, the middle orbit is neutrally stable, so the φ_{conv} measure does not make sense. This speed of convergence also gives a measure of the contraction mapping associated with the periodic solutions of the system.

We calculate the critical shrinking of the normalized interval between adjacent spikes η_{crit} as follows:

$$\eta_{\text{crit}} \equiv \frac{\min\limits_{x_0 \in (x_{\min}, x_{\max})} \tau_1(x_0)}{\tau_1(x_m)}. \tag{34}$$

In the numerator we have a minimal interval between adjacent spikes such that the system does not leave the sustained spiking mode, and in the denominator we have the interval between adjacent spikes $\tau_1(x_m)$ calculated on the limit cycle or middle orbit. As the limit cycle or middle orbit corresponds to antiphase firing, $\tau_1(x_m)$ equals half of the interspike interval. Consequently, the normalization by $\tau_1(x_m)$ in (34) accounts for possible changes in the antiphase single neuron ISI caused by a change of parameters, leaving the pure effect of synchronization between spikes of different neurons.

III. RESULTS

A. Background: solution geometry for an uncoupled system

We start our analysis from the system of two uncoupled QIF neurons ($I_{\text{syn}} = 0$). We do it in order to describe the direction field on the phase plane, because our results suggest that its main features remain the same after adding synaptic interaction. Since the coupling we introduce is fast and depends on the spikes of the neurons, the uncoupled vector fields form a scaffold for the coupled case: Most of the characteristic solutions are preserved together with the nodes and the saddles with their separatrices. Understanding the geometry of this direction field will enable us to pursue analysis of the full system below. Obviously, the neurons are independent in this case. The constant external current is inhibitory ($I_{\text{ext}} < 0$), so both neurons are excitable. Given the initial state (x_0, y_0), the system has the following solution:

$$\begin{aligned} x(t) &= \phi^{\text{ex}}_{I_{\text{ext}}}(x_0, t), \\ y(t) &= \phi^{\text{ex}}_{I_{\text{ext}}}(y_0, t), \end{aligned} \tag{35}$$

where the function ϕ is given by (4).

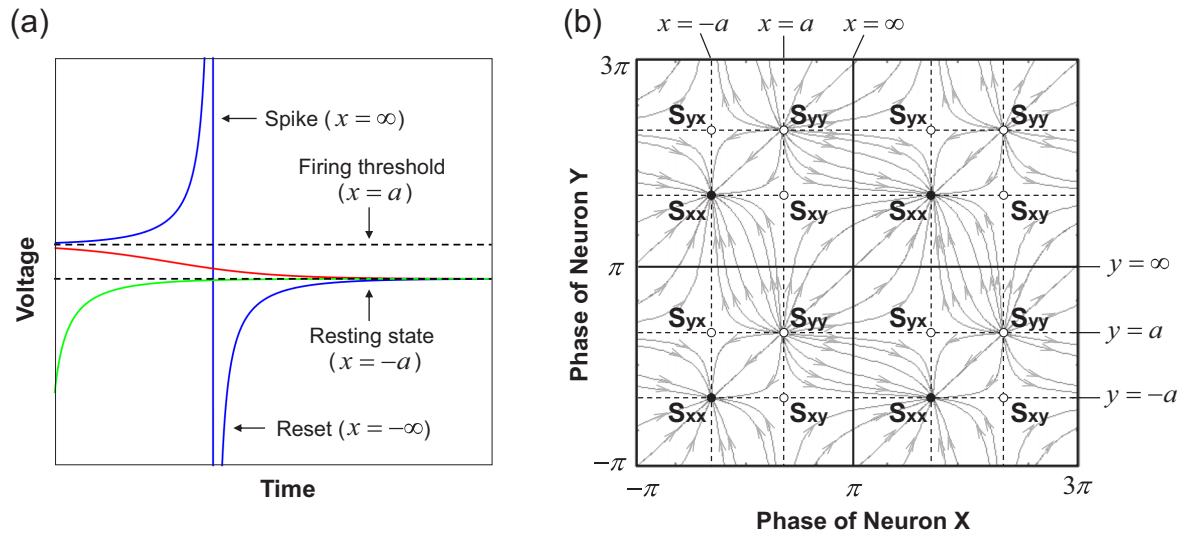

FIG. 1. (a) Dynamics of voltage of a single QIF neuron. Solid lines represent the orbits that start from the different voltages. Dashed lines represent the resting state and the threshold. (b) Phase portrait of uncoupled system. Black dot: stable fixed point; white dots: unstable fixed points. Dashed black lines represent firing thresholds (separatrices of the saddle points); solid black lines represent the phases at which spikes occur. Four periods of a system are shown.

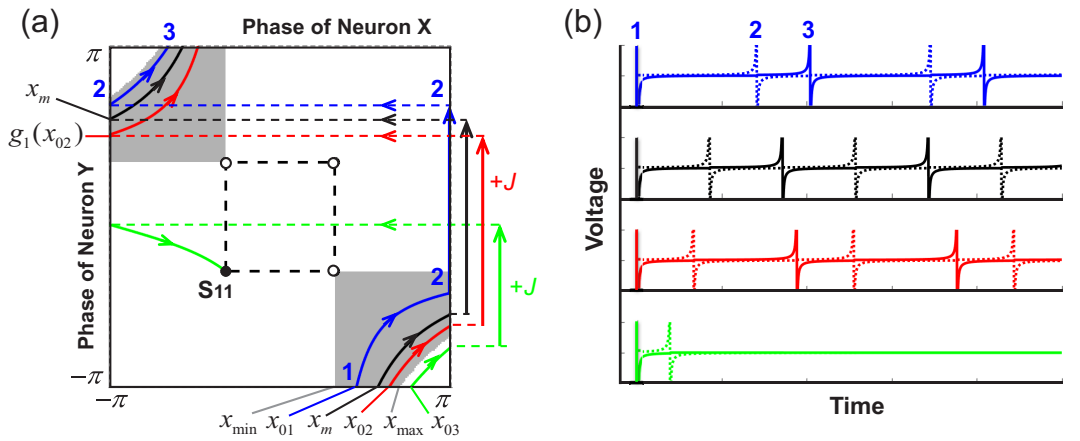

FIG. 2. (a) Phase portrait of a system with instant synapse ($I_{\text{ext}} = -0.3$, $J = 2.5$). Gray regions: active state; corners of the dashed square are fixed points of the system. Blue (starting from x_{01}), red (starting from x_{02}), and green (starting from x_{03}) solid lines: arbitrary orbits; black (starting from x_m) solid line: "middle orbit." Vertical arrows represent instantaneous increase of voltage of neuron Y by J after a spike of neuron X. Horizontal dashed lines represent the phase switching from π to $-\pi$ (which are equivalent on a torus). Blue, black, and red orbits (starting from x_{01}, x_m, and x_{02}, respectively) correspond to infinite spike trains, while the green orbit (starting from x_{03}) converges to the subthreshold resting state. Numerals 1–3 denote the moments of the first three spikes on the blue orbit (starting from x_{01}). (b) Spike trains corresponding to the orbits from (a). Solid lines: voltage dynamics of neuron Y; dashed lines: voltage dynamics of neuron X.

The solution for neuron X is represented in Fig. 1(a). If $x_0 < a$, then voltage converges to $x = -a$. If $x_0 > a$, then voltage goes to infinity (producing a spike), resets to minus infinity, and, again, converges to $x = -a$. Thus $x = a$ is the threshold of spike generation, and $x = -a$ is the resting state.

The time of the spike can be expressed as

$$\tau_1(x_0) = \tilde{T}^{\text{ex}}_{I_{\text{ext}}}(x_0), \tag{36}$$

where the function $\tilde{T}$ is given by (10).

The phase portrait of the system (35) is represented at Fig. 1(b). The system has four fixed points:

$$\begin{aligned} S_{11} &= (-a, -a), \quad S_{12} = (a, -a), \\ S_{21} &= (-a,a), \quad S_{22} = (a,a), \end{aligned} \tag{37}$$

where S_{11} is a stable node, S_{22} is an unstable node, and S_{12} and S_{21} are saddles. S_{11} corresponds to the steady state of the system, in which both neurons are at their resting potentials. The fixed points are connected by the separatrices of the saddle points S_{12} and S_{21}; these separatrices correspond to the thresholds, above which one of the neurons fires a spike.

B. System with instant synapse

Now we continue our analysis and consider a system of two QIF neurons with instant excitatory coupling. The dynamics of this system is equivalent to the dynamics of the uncoupled system, except for the fact that each neuron receives a voltage step when another neuron fires a spike:

$$\begin{aligned} \frac{dx}{dt} &= x^2 + I_{\text{ext}} + I^x_{\text{syn}}, \\ \frac{dy}{dt} &= y^2 + I_{\text{ext}} + I^y_{\text{syn}}, \\ x &\leftarrow -\infty, \quad y \leftarrow y + J \quad \text{if} \quad x = \infty, \\ y &\leftarrow -\infty, \quad x \leftarrow x + J \quad \text{if} \quad y = \infty, \end{aligned} \tag{38}$$

while in the time intervals between spikes, the solution is given by (35).

The phase portrait of the system is presented in Fig. 2(a). The gray color represents the region of activity: If an orbit starts somewhere in this region, then the system stays in the active state, and produces an infinite train of spikes. If an orbit starts outside the gray region, it converges to the subthreshold fixed point S_{11}, so the system settles down to the background resting state. The corresponding spike trains are presented in Fig. 2(b).

Now we derive an analytical description of the behavior of the system in the activity region. Let $(x_0, -\infty)$ be the initial state of the system. Obviously, neuron X will produce a spike only if $x_0 > a$ (recall that a is the firing threshold). We can get the expression for the time of this spike from (36)

$$t_x = \tau_1(x_0) = \frac{1}{a}\text{arctanh}\frac{a}{x_0}. \tag{39}$$

In the time interval $0 < t < t_x$, the solution is given by (35). At the time $t = t_x$, we get

$$\begin{aligned} b(t_x) = x_0; \quad y_1 &= g_1(x_0) = J + f(-\infty,t_x) \\ &= J - b(t_x) = J - x_0. \end{aligned} \tag{40}$$

Neuron Y will produce the second spike only if

$$y_1 = g_1(x_0) > a, \tag{41}$$

or, equivalently,

$$x_0 < J - a. \tag{42}$$

The voltage of neuron X after the second spike of neuron Y is given by

$$g_2(x_0) = g_1(J - x_0) = x_0. \tag{43}$$

Thus, for any $x_0 \in (a, J - a)$, the orbit of a point $(x_0, -\infty)$ is a cycle, and, because $|dg_2/dx_0| = 1$, this cycle is neutrally stable. Evidently, any such cycle corresponds to an infinite

spike train, and thus it lies inside the region of persistent activity on the phase plane [e.g., blue, black, and red orbits in Fig. 2(a), starting from x_{01}, x_m, and x_{02}, respectively]. If $x_0 \notin (a, J-a)$, then the orbit of $(x_0, -\infty)$ converges to the resting state, producing a maximum of one spike before this [e.g., green orbit in Fig. 2(a), starting from x_{03}]. Consequently,

$$x_{\min} = a, \quad x_{\max} = J - a, \tag{44}$$

and the width of the activity region is given by

$$D_{\text{act}} \equiv x_{\max} - x_{\min} = J - 2a. \tag{45}$$

Obviously, the region of activity exists only if

$$x_{\min} < x_{\max} \Leftrightarrow J > 2a, \tag{46}$$

i.e., when synaptic coupling is strong enough compared with tonic inhibition.

Consider that an external influence perturbs a state of the system that is initially in the region of persistent activity. When synaptic coupling is stronger, and tonic inhibition is weaker, the width of the region of activity, given by (45), is larger, so the external perturbations are less likely to push the system away from this region and switch it from the active to the quiescent state.

Among the neutrally stable cycles mentioned above, there is one special "middle" cycle that contains a state given by the fixed point of g_1:

$$g_1(x_m) = x_m\,. \tag{47}$$

From (47) and (40) we obtain

$$x_m = J/2. \tag{48}$$

This "middle" orbit corresponds to the spike train, in which all the intervals between adjacent spikes of neurons X and Y are the same [Fig. 2(b), black trace (second panel from the top)]. All other orbits that lie inside the activity region correspond to the spike trains with alternating short and long intervals between adjacent spikes of the two neurons [Fig. 2(b), blue and red traces (first and third panels from the top, respectively)]. Long intervals correspond to the parts of the orbit that pass close to one of the saddle points [S_{12} or S_{21}; see Fig. 2(a), segment 1–2 of the blue orbit (starting from x_{01}), and Fig. 2(b), segment 1–2 of the blue trace (first panel from the top)]; short intervals correspond to the parts of the orbit that pass near the curved border of the activity region [Fig. 2(a), segment 2–3 of the blue orbit (starting from x_{01}), and Fig. 2(b), segment 2–3 of the blue trace (first panel from the top)]. If an interval between adjacent spikes is too small, then the corresponding segment of the orbit passes near the curved border of the activity region, but from the outside of this region, so further spiking activity is terminated [Fig. 2(a), green orbit (starting from x_{03}), and Fig. 2(b), green trace (bottom pannel)]. The critical shrinking of the interval between adjacent spikes can be expressed as follows:

$$\eta_{\text{crit}} = \frac{\tau_1(x_{\max})}{\tau_1(x_m)} = \frac{\operatorname{arctanh}[a/(J-a)]}{\operatorname{arctanh}[2a/J]}. \tag{49}$$

We note that the interspike interval for orbits passing near the border of the activity region is longer than the interspike interval for the middle orbit [compare the interval between spikes 1 and 3 in Fig. 2(b) for the black trace (middle orbit; second panel from the top) and for the red and blue traces (orbits near the border; third and first panels from the top, respectively)]. It means that shrinking of $\tau_1(x_{\max})$ compared to $\tau_1(x_m)$ is not a consequence of an instantaneous increase of firing rate, so η_{crit} actually is a measure of partial synchronization between neurons. The dependence of η_{crit} on J for two different values of I_{ext} is represented in Fig. 3. Consider that the system is on the "middle" orbit, and that a hypothetical external perturbation tends to synchronize the neurons. From Fig. 3, we can see that in the case of weaker tonic inhibition and stronger synaptic coupling, a stronger spike synchronization can be tolerated by the circuit before spiking activity is destroyed, so the active state of the system is more robust to the external synchronizing perturbation in this case. Therefore, the closer the two neurons are to their respective saddle-node bifurcations, the more tolerant is the sustained activity in the circuit to partial synchronization by a common input. The same goes for stronger recurrent coupling.

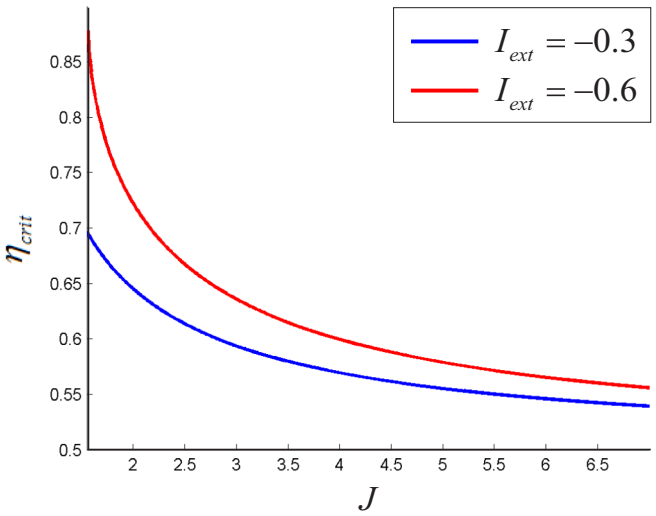

FIG. 3. Dependence of critical shrinking of interval between adjacent spikes (η_{crit}) on synaptic weight (J) for two different levels of tonic inhibition (I_{ext}) in the system with instant synaptic interaction.

C. System with square synaptic kernel

Now we analyze the behavior of a system of two coupled QIF neurons with square synaptic kernels. While artificial, we will see in the subsequent section that this type of coupling gives a qualitatively similar phase-plane structure to a more realistic exponential synaptic time course, yet allows us to do some analytics for the critical spike-time shifts. In this system, a neuron receives constant synaptic current J during the time interval τ_s after a spike of another neuron, while at all other time moments the synaptic current is zero. Assuming that τ_s is smaller than the typical time interval between adjacent spikes of two neurons, we can use (22) and consider the following autonomous system:

$$\frac{dx}{dt} = x^2 + I_{\text{ext}} + Jh(x_s - x),$$
$$\frac{dy}{dt} = y^2 + I_{\text{ext}} + Jh(x_s - y),$$

$$x \leftarrow -\infty \text{ if } x = \infty,$$
$$y \leftarrow -\infty \text{ if } y = \infty, \tag{50}$$

where $h(\cdot)$ is the Heaviside function, and x_s is the voltage that a neuron reaches after time τ_s since it fired a spike (assuming that input synaptic current to the neuron is zero during this time interval):

$$x_s = \phi^{\text{ex}}_{I_{\text{ext}}}(-\infty, \tau_s) = -\frac{a}{\tanh(a\tau_s)}. \tag{51}$$

Self-sustained spiking activity is possible in this system only if synaptic input can push the postsynaptic neuron across its bifurcation and switch it from the excitable state to the oscillatory state, because during the influence of this input, the neuron should increase its voltage from $x < -a$ to $x > a$, while in the excitable state, the voltage can only decrease in the $x \in (-a\,; a)$ interval. Thus, in the presence of synaptic input, the total input current to a neuron should be positive, which gives us the following condition:

$$J > |I_{\text{ext}}|. \tag{52}$$

Consider that the system evolves from a state $(x_0; y_0)$ to a state $(x; y)$ in a time t, and that no spikes are produced during this evolution. The exact form of the solution depends on which neurons receive nonzero synaptic input: none of them, only one, or both. Thus there are four possible cases.

(a) $x_0, x \geqslant x_s$; $y_0, y \geqslant x_s$.

The synaptic activity is absent, so both neurons are excitable:

$$x(t) = \phi^{\text{ex}}_{I_{\text{ext}}}(x_0, t) = -b_{\text{ex}} + \frac{{b_{\text{ex}}}^2 - a^2}{b_{\text{ex}} - x_0},$$
$$y(t) = \phi^{\text{ex}}_{I_{\text{ext}}}(y_0, t) = -b_{\text{ex}} + \frac{{b_{\text{ex}}}^2 - a^2}{b_{\text{ex}} - y_0},$$
$$b_{\text{ex}} = \frac{a}{\tanh(at)}. \tag{53}$$

(b) $x_0, x \geqslant x_s$; $y_0, y < x_s$.

Neuron Y recently fired a spike, and it produces an input synaptic current to neuron X. Thus neuron Y is excitable, and X is oscillatory:

$$x(t) = \phi^{\text{osc}}_{I_{\text{ext}}+J}(x_0, t) = -b_{\text{osc}} + \frac{{b_{\text{osc}}}^2 + \tilde{a}^2}{b_{\text{osc}} - x_0},$$
$$y(t) = \phi^{\text{ex}}_{I_{\text{ext}}}(y_0, t) = -b_{\text{ex}} + \frac{{b_{\text{ex}}}^2 - a^2}{b_{\text{ex}} - y_0},$$
$$\tilde{a} = \sqrt{J - a^2}, \quad b_{\text{osc}} = \frac{\tilde{a}}{\tan(\tilde{a}t)}, \quad b_{\text{ex}} = \frac{a}{\tanh(at)}. \tag{54}$$

(c) $x_0, x < x_s$; $y_0, y \geqslant x_s$.

Neuron X recently fired a spike, so X is excitable, and Y is oscillatory.

This case is equivalent to (b) if we interchange X and Y.

(d) $x_0, x < x_s$; $y_0, y < x_s$

Both neurons recently fired spikes, so both of them are oscillatory:

$$x(t) = \phi^{\text{osc}}_{I_{\text{ext}}+J}(x_0, t) = -b_{\text{osc}} + \frac{{b_{\text{osc}}}^2 + \tilde{a}^2}{b_{\text{osc}} - x_0},$$
$$y(t) = \phi^{\text{osc}}_{I_{\text{ext}}+J}(y_0, t) = -b_{\text{osc}} + \frac{{b_{\text{osc}}}^2 + \tilde{a}^2}{b_{\text{osc}} - y_0},$$
$$\tilde{a} = \sqrt{J - a^2}, \quad b_{\text{osc}} = \frac{\tilde{a}}{\tan(\tilde{a}t)}. \tag{55}$$

Note that in case (d) our assumption of a large interval between adjacent spikes is not satisfied, so moving from time-dependent to phase-dependent coupling kernels using (22) may change the behavior of the system.

In the expressions above, the functions ϕ^{osc} and ϕ^{ex} were taken from (6) and (4), respectively. These expressions are valid only in the time intervals between events: spikes and terminations of synaptic activity; at the moments of events one should switch from one system of equations to another.

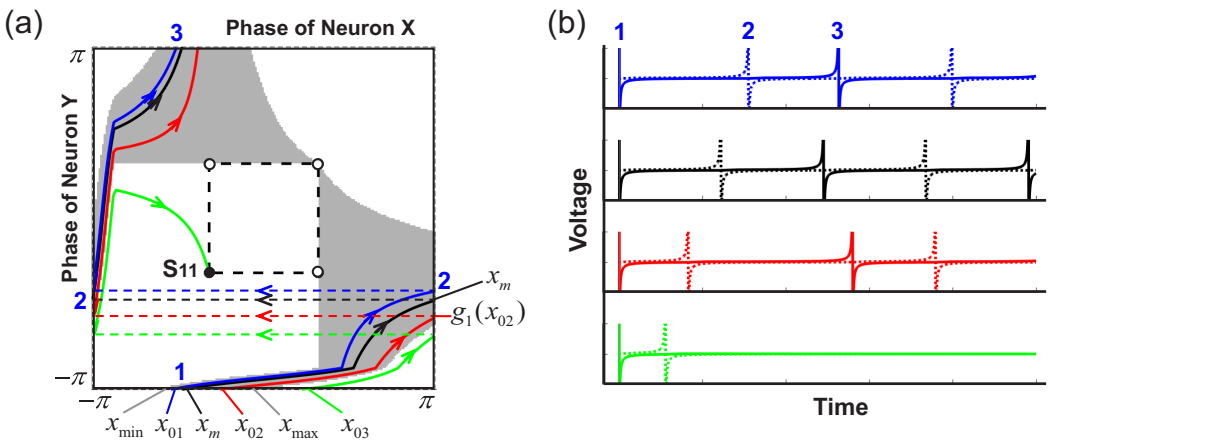

FIG. 4. (a) Phase portrait of a system with square synapse ($I_{\text{ext}} = -0.3$, $J = 10$, $\tau_s = 0.2$). Gray regions: active state; corners of the dashed square are fixed points of the system. Blue (starting from x_{01}), red (starting from x_{02}), and green (starting from x_{03}) solid lines: arbitrary orbits; black (starting from x_m) solid line: limit cycle. Horizontal dashed lines represent the phase switching from π to $-\pi$ (which are equivalent on a torus). Blue, black, and red orbits (starting from x_{01}, x_m, and x_{02}, respectively) correspond to infinite spike trains, while the green orbit (starting from x_{03}) converges to the subthreshold resting state. Numerals 1–3 denote the moments of the first three spikes on the blue orbit (starting from x_{01}). (b) Spike trains corresponding to the orbits from (a). Solid lines: voltage dynamics of neuron Y; dashed lines: voltage dynamics of neuron X.

The phase portrait of the system with several orbits is represented in Fig. 4(a), and the spike trains that correspond to these orbits, in Fig. 4(b) [the legend is the same as in Figs. 2(a) and 2(b), respectively]. There are some notable differences with the previous case considered. At the bottom of the phase plane we can see a long, thin, nearly horizontal "wing" of the gray region. This wing corresponds to the situation in which neuron Y just fired a spike, so neuron X receives input current, and its voltage grows very fast. The analogous region at the left side of the phase portrait corresponds to the situation in which neuron X just fired a spike and neuron Y receives input current. If we transiently partially synchronize the spikes (e.g., advance a spike of one neuron by a weak transient excitatory input), the system will shift out of the gray wing and fall into the white region, subsequently converging to the double-rest point; see the green orbit (starting from x_{03}) in Fig. 4(a).

As in the case of instant coupling, we analytically describe behavior of the system in the region of self-sustained activity. Let us assume that the system starts from the point $(x_0, -\infty)$ that corresponds to the spike of neuron Y, and that $x_0 > x_s$. A spike of neuron X can occur only if the voltage x after the termination of synaptic input is above the threshold a. This gives us the following condition for the minimal value of x_0 (denoted as $x_{\min}$) that leads to a spike:

$$\phi^{\mathrm{osc}}_{I_{\mathrm{ext}}+J}(x_{\min},\tau_s) = a. \tag{56}$$

From this condition, we can express $x_{\min}$ in the following way:

$$x_{\min} = b_s - \frac{{b_s}^2+\tilde{a}^2}{b_s+a},\quad b_s = \frac{\tilde{a}}{\tan(\tilde{a}\tau_s)},$$
$$\tilde{a} = \sqrt{J-a^2}. \tag{57}$$

It should be noted that the statement above is valid only if $x_{\min} > x_s$.

State of the system at the moment τ_s is expressed as follows:

$$\hat{x}_0 = \phi^{\mathrm{osc}}_{I_{\mathrm{ext}}+J}(x_0,\tau_s),$$
$$\hat{y}_0 = x_s. \tag{58}$$

Time from the termination of synaptic input to the spike of neuron X is given by

$$\hat{t}_0 = T^{\mathrm{ex}}_{I_{\mathrm{ext}}}(\hat{x}_0,\infty) = \frac{1}{a}\operatorname{arctanh}\frac{a}{\hat{x}_0}, \tag{59}$$

where the function T^{ex} is given by (5).

Voltage of neuron Y during the spike of neuron X is given by

$$y_1 = \phi^{\mathrm{ex}}_{I_{\mathrm{ext}}}(\hat{y}_0,\hat{t}_0) = -\hat{b}_0 + \frac{\hat{b}_0^2-a^2}{\hat{b}_0-\hat{y}_0},\quad \hat{b}_0 = \frac{a}{\tanh(a\hat{t}_0)}. \tag{60}$$

By substituting (58) and (59) into (60), we obtain the following spike-to-spike voltage mapping:

$$y_1 \equiv g_1(x_0) = -\hat{x}_0 + \frac{\hat{x}_0^2-a^2}{\hat{x}_0-x_s}$$
$$= \frac{(a^2+b_sx_s)x_0 - (a^2b_s-\tilde{a}x_s)}{(b_s+x_s)x_0+(\tilde{a}^2-b_sx_s)}. \tag{61}$$

The inverse mapping can be expressed as follows:

$$x_0 \equiv g_1^{-1}(y_1) = \frac{(b_sx_s-\tilde{a}^2)y_1+(\tilde{a}^2x_s-a^2b_s)}{(x_s+b_s)y_1-(a^2+b_sx_s)}. \tag{62}$$

The second spike of neuron Y can occur only if

$$y_1 = g_1(x_0) > x_{\min}, \tag{63}$$

where $x_{\min}$ is given by (57). This gives us the maximal value of x_0 (denoted as $x_{\max}$) that leads to the second spike:

$$x_{\max} = g_1^{-1}(x_{\min}). \tag{64}$$

Thus the necessary condition of the activity region existence on the phase plane is

$$x_{\min} < x_{\max}, \tag{65}$$

where $x_{\min}$ and $x_{\max}$ are given by (57) and (64), respectively.

There is a limit cycle that corresponds to the fixed point of g_1 (and, therefore, of g_2):

$$x_m = g_1(x_m). \tag{66}$$

Using the expression (61) for g_1, one can get x_m as the solution of the quadratic equation:

$$K_1x^2 - K_2x + K_3 = 0,$$
$$K_1 = x_s+b_s,$$
$$K_2 = 2b_sx_s + a^2 - \tilde{a}^2,$$
$$K_3 = a^2b_s - \tilde{a}^2x_s. \tag{67}$$

Our numerical simulation had shown that the larger root of this equation corresponds to the observed limit cycle:

$$x_m = \frac{K_2+\sqrt{K_2^2-4K_1K_3}}{2K_1}. \tag{68}$$

From (61), the speed of convergence to the limit cycle can be expressed as follows:

$$\varphi_{\mathrm{conv}} = \left[\left.\frac{dg_1(x_0)}{dx_0}\right|_{x_m}\right]^{-1} = \frac{[x_m(b_s+x_s)+(\tilde{a}^2-x_sb_s)]^2}{(a^2-x_s^2)(b_s^2+\tilde{a}^2)}. \tag{69}$$

The plot of φ_{conv}, obtained for several combinations of parameters, is represented in Fig. 5(a). We can see that $\varphi_{\mathrm{conv}} > 1$ for all considered cases, which means that all orbits that start from $(x_0, -\infty)$ such that $x_0 \in (x_{\min},x_{\max})$ converge to the limit cycle; i.e., the limit cycle is stable. It is also seen that the convergence is faster when synaptic coupling (given by $J\tau_s$) is stronger, and the synaptic time constant (τ_s) is larger. Surprisingly, the convergence is faster when the tonic inhibition (I_{ext}) is stronger; however, this effect is quite subtle.

Plots of the activity region width D_{act} and of the critical shrinking of the interval between adjacent spikes η_{crit} [given by (31) and (34)] obtained for various combinations of parameters are represented in Figs. 5(b) and 5(c), respectively. As expected, we can see that the activity region is wider, and the critical time interval is smaller, when the synaptic interaction is stronger and slower and the tonic inhibition is weaker.

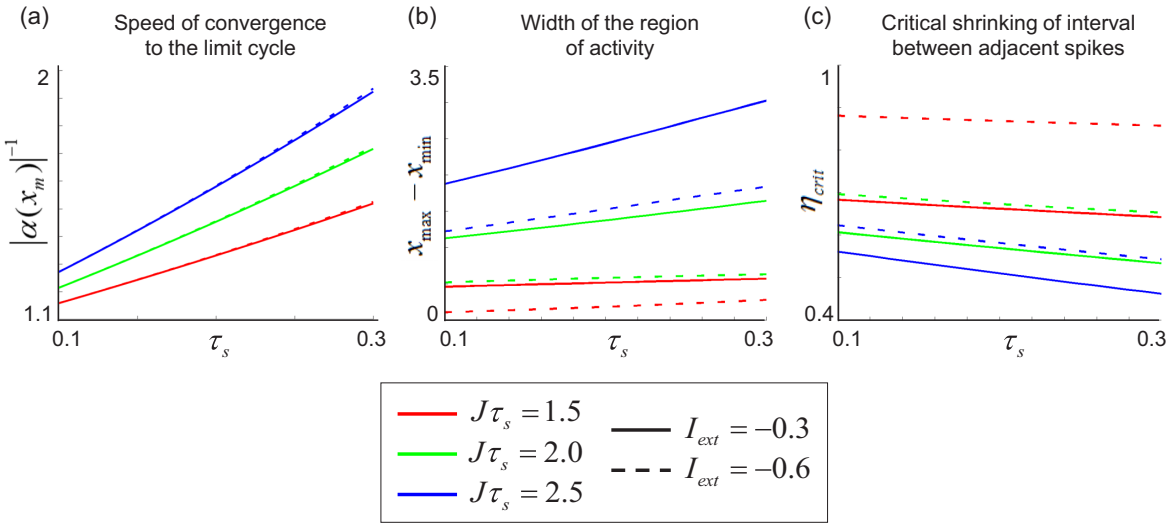

FIG. 5. Three metrics of the active-state robustness in the system with square synaptic kernel, plotted versus synaptic time constant τ_s for various values of tonic inhibition I_{ext} and synaptic coupling $J\tau_s$: speed of convergence to the limit cycle (a); width of the activity region (b); critical shrinking of interval between adjacent spikes that does not destroy self-sustained activity (c).

D. System with exponential synaptic kernel

In this section, we perform numerical analysis of a system with an exponential synaptic kernel and compare the results of this analysis with the previously described results obtained for the system with a less realistic square kernel. As before, we assume that τ_s is smaller than the typical time interval between adjacent spikes, and use (22) to get an autonomous system:

$$\frac{dx}{dt} = x^2 + I_{\text{ext}} + J\exp\left[-\frac{\tilde{T}^{\text{ex}}_{I_{\text{ext}}}(y)}{\tau_s}\right],$$
$$\frac{dy}{dt} = y^2 + I_{\text{ext}} + J\exp\left[-\frac{\tilde{T}^{\text{ex}}_{I_{\text{ext}}}(x)}{\tau_s}\right],$$
$$x \leftarrow -\infty \text{ if } x = \infty,$$
$$y \leftarrow -\infty \text{ if } y = \infty, \tag{70}$$

where the function $\tilde{T}$ is given by (10).

The phase portrait of the system and several spike trains are represented in Fig. 6. The results are qualitatively similar to the ones obtained for the system with a square kernel (see Fig. 4): One can see the activity region (gray) of approximately the same shape, and the limit cycle (black curve, starting from x_m) that attracts all other orbits from the activity region. Numerically obtained plots of metrics of the active-state robustness (speed of convergence to the limit cycle; width of the activity region; critical shrinking of interval between adjacent spikes) are represented in Fig. 7. These plots are qualitatively similar to the ones presented in Fig. 5 for the

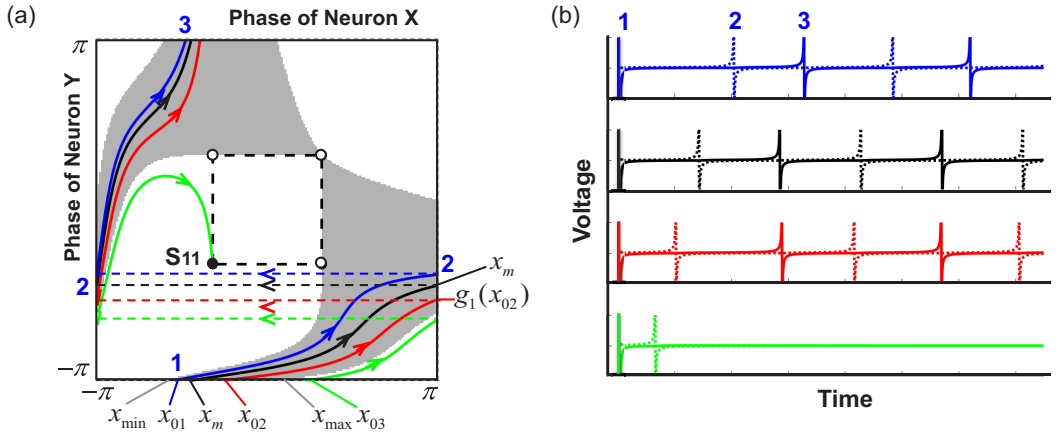

FIG. 6. (a) Phase portrait of a system with voltage-dependent exponential synapse ($I_{\text{ext}} = -0.3$, $J = 10$, $\tau_s = 0.2$). Gray regions: active state; corners of the dashed square are fixed points of the system. Blue (starting from x_{01}), red (starting from x_{02}), and green (starting from x_{03}) solid lines: arbitrary orbits; black (starting from x_m) solid line: limit cycle. Horizontal dashed lines represent the phase switching from π to $-\pi$ (which are equivalent on a torus). Blue, black, and red orbits (starting from x_{01}, x_m, and x_{02}, respectively) correspond to infinite spike trains, while the green orbit (starting from x_{03}) converges to the subthreshold resting state. Numerals 1–3 denote the moments of the first three spikes on the blue orbit (starting from x_{01}). (b) Spike trains corresponding to the orbits from (a). Solid lines: voltage dynamics of neuron Y; dashed lines: voltage dynamics of neuron X.

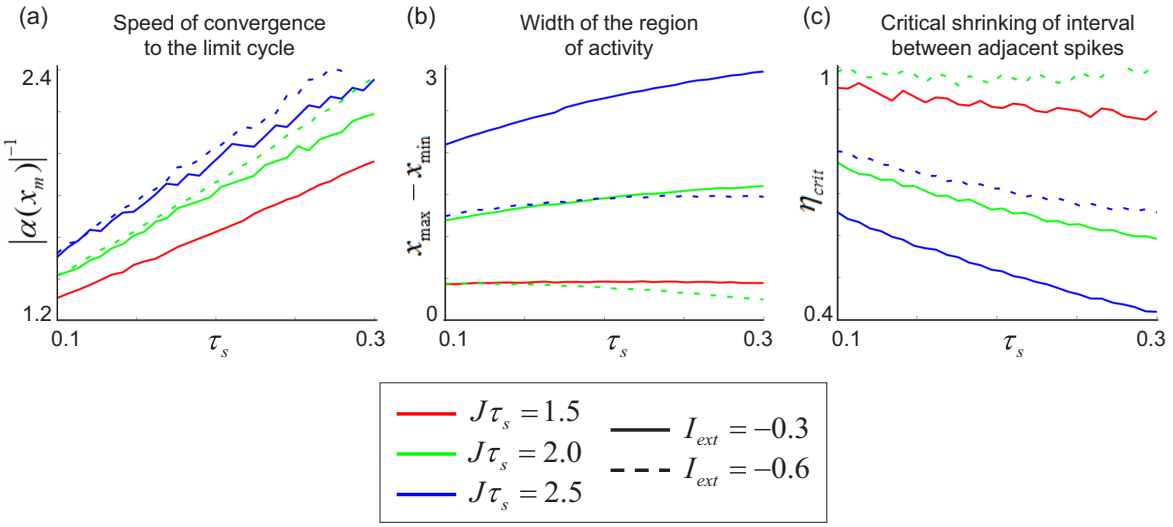

FIG. 7. Three metrics of the active-state robustness in the system with exponential synaptic kernel, plotted versus synaptic time constant τ_s for various values of tonic inhibition I_{ext} and synaptic coupling $J\tau_s$: speed of convergence to the limit cycle (a); width of the activity region (b); critical shrinking of interval between adjacent spikes that does not destroy self-sustained activity (c).

system with a square kernel: The active state is more robust when tonic inhibition is weaker, and synaptic interaction is stronger and slower. The plots for $I_{\text{ext}} = -0.6$, $J\tau_s = 1.5$ are not presented because the activity region is so small in this case that our numerical algorithm failed to calculate the metrics of the active-state robustness.

In order to further check our findings, we performed numerical simulations for the system with a delayed exponential synaptic kernel and for the system with a synapse with a finite-rise-time kernel described by an alpha function. We found that the phase portraits of these systems do not differ qualitatively from the results described above (simulations not shown).

IV. DISCUSSION AND CONCLUSIONS

In the present study, we analyzed the behavior of a system of two excitable quadratic integrate-and-fire neurons; the system is bistable and can be considered as a minimal model for a circuit that maintains a memory trace of an item to be used in a delayed response task (or working memory task): It has a quiescent background state and an active regime characterized by self-sustained spiking activity based on mutual synaptic excitation between the neurons. The active regime is initiated by a transient excitatory stimulus and is antisynchronous. It can be stopped by a transient stimulus rapidly. The constituent neurons in this minimal circuit were modeled by the quadratic integrate-and-fire equations, that are a normal form for the saddle-node bifurcation and a canonical model for type I excitability. The coupling was excitatory and modeled fast glutamatergic synapses. The main goal of our study was to see how robust the persistent activity can be to transient perturbations in the spike times away from the stable antisynchrony. We considered an uncoupled system, as well as systems of neurons coupled via excitatory synapses with either a delta pulse, square, or exponential kernel. We developed the expressions for synaptic currents in such a way that they depend only on the voltage of a fired neuron, but not explicitly on the time since the last spike. Thus all systems under consideration were two-dimensionally autonomous, which allowed us to perform phase-plane analysis.

In accordance with the previous work [6], we found that the uncoupled system has four equilibria: a stable node (both neurons are at their resting potentials), two saddle points (one of the neurons is at its resting potential, and the other one is at its firing threshold), and an unstable node (both neurons are at their firing thresholds). For the coupled systems with strong enough synaptic coupling, in addition to the subthreshold equilibrium, we characterized an invariant "butterfly" shaped region on the phase plane that corresponds to self-sustained spiking activity. Any orbit that starts from this region corresponds to an infinite spike train in which two neurons fire alternatively, pushing each other across the firing threshold. For the system with instant coupling, the region of activity was fully located inside the phase-plane quadrants in which the voltage of one neuron is above the firing threshold, and the voltage of another one is below the resting potential. For the systems with noninstant coupling (via square and exponential synapses), the region of activity extended outside the quadrants mentioned above—forming thin "wings" of the butterfly. In the latter case, the geometry of the activity region is similar to the one discovered by Gutkin *et al.* [6] for a different type of synaptic kernel.

Orbits that pass inside the region of activity correspond to spike trains with relatively small synchrony (or strong antiphase) between the neurons. These antiphase spike trains in a two-neuron system are equivalent to the splay state [8] observed in larger networks. Pushing the system toward one of the borders of the activity region leads to partial synchronization: Some intervals between subsequent spikes become shorter, and the others longer. Perturbing the system out of the activity region terminates spiking activity: It leads either to convergence to the subthreshold equilibrium without firing spikes, or to firing one more spike very soon after the previous one, followed again by convergence to the equilibrium. Thus a critical level of synchronization (related to the interval between adjacent spikes) exists, above which

the system switches from the active state to the background state. This result is in agreement with the idea that sustained spiking activity that reflects maintenance of information in working memory models can be terminated by an excitatory pulse that synchronizes the neural population [17]. However, in that work, strong perturbation ensuring hard synchrony was considered. Here we show that the pulse can be much weaker, depending on the coupling strength, the temporal scale of the synapses, and the distance of the neurons from their individual bifurcation points.

The main goal of the present study was to analyze robustness of the active state. For the system with instant synaptic interaction, we proved that all orbits in the activity region are neutrally stable; for the systems with noninstant interaction, we have found the existence of a limit cycle that attracts all orbits that start within the activity region. These findings are in agreement with the study [8] in which results were obtained for stability of the splay state in the network of excitatory neurons. In this work we went beyond that study, since we assessed robustness of the active state using three metrics: (a) speed of convergence to the limit cycle (given by the inverse of the absolute value of the spike-to-spike voltage mapping derivative at the fixed point); (b) width of the activity region (along a line that corresponds to firing a spike by one of the neurons); (c) critical shrinking of the interval between adjacent spikes (relative to the interval observed in the antiphase regime) that does not lead to termination of spiking activity. We note that normalization of metric (c) by the interval obtained in the antiphase regime guarantees that changes of this metric caused by changes of model parameters are not related to changes in the steady-state firing rate and thus reflect the critical synchronization itself. For the system with instant synapses, we showed that metrics (b) and (c) are larger (so the active state is more robust) when the tonic inhibition is weaker and the synaptic coupling is stronger [metric (a) cannot be calculated in this case because the system does not have a limit cycle]. For the system with a square kernel, we derived analytical expressions for all three metrics and found that (a), (b), and (c) are larger when the tonic inhibition is weaker, the synaptic coupling is stronger, and the synaptic decay is slower. Interestingly, metric (a) depended very weakly on the level of tonic inhibition. Dependence of the robustness metrics on the synaptic decay time constant supports the idea that self-sustained activity can be stabilized by adding slow synapses to a model [18]. All the aforementioned findings were reproduced in the more realistic case of an exponential synaptic kernel, for which we calculated the robustness metrics numerically. Interestingly, robustness of the sustained activity in the circuit can also be improved by decreasing the tonic "inhibitory" current. This could be done physiologically by a number of potential mechanisms, for example, downregulating slow hyperpolarizing currents that are quasitonically active at rest potentials (the leak currents, or the dopaminergic or cholinergic modulation of the M-type potassium current) or activity-dependent changes in the reversal potentials of GABA-mediated inhibitory synapses [19–21].

In summary, we investigated the behavior of a bistable two-neuron system that can serve as a minimal model of a working memory circuit. We performed phase-plane analysis and defined the geometry of a region of self-sustained spiking activity, extending the previously obtained results [6]. We confirmed the idea that self-sustained activity can be terminated by synchronization of neuronal activities. Finally, we explored how robustness of the active state depends on the model parameters; in the cases of instant and square synapses, we did it analytically. The results we presented here give an analytical basis for the phenomena we observed by simulation in larger scale networks. For example, we saw that persistent activity in a large network supporting spatial working memory is asynchronous and is turned off by synchronization [17]. We also saw that in a large network model of discrete working memory, the persistent activity encoding the memory trace could be turned off by correlated noise with the probability of turning off being controlled by the coherence of the noise [14]. We conjectured that this effect is due to partial synchronization within the large network. Interestingly, as opposed to [9], our work proves that the turnoff does not require recruitment of inhibition. Hence our results fall into a hypothesis suggesting that glutamatergic mechanisms may be sufficient to implement dynamical control of sustained activity in working memory tasks [14]. In the future, we are planning to analyze the behavior of the systems considered in this paper in the presence of periodic external input, and to find out how parameters of this input affect robustness of the active state, as it was made for the network of excitatory neurons in [14]. We are also planning to analyze the system with excitatory random noise, in order to prove that the previously observed inverse stochastic resonance effect [22,23] is related to the partial-synchronization-dependent quenching we explored here.

ACKNOWLEDGMENTS

This work was done at the National Research University Higher School of Economics, Moscow by Nikita Novikov and Boris Gutkin and was financially supported by the Russian Ministry of Education (Contract No. 14.608.21.0001, unique ID Project No. RFMEFI60815X0001).

[1] P. S. Goldman-Rakic, Neuron **14**, 477 (1995).
[2] S. Funahashi, C. J. Bruce, and P. S. Goldman-Rakic, J. Neurophysiol. **61**, 331 (1989).
[3] J. M. Fuster and G. E. Alexander, Science **173**, 652 (1971).
[4] G. Major and D. Tank, Curr. Opin. Neurobiol. **14**, 675 (2004).
[5] D. J. Amit and N. Brunel, Cereb. Cortex **7**, 237 (1997).
[6] M. Dipoppa, M. Krupa, A. Torcini, and B. S. Gutkin, SIAM J. Appl. Dyn. Syst. **11**, 864 (2012).
[7] B. Gutkin, T. Hely, and J. Jost, Neurocomputing **58-60**, 753 (2004).
[8] C. R. Laing and C. C. Chow, Neural Comput. **13**, 1473 (2001).

[9] A. Compte, N. Brunel, P. S. Goldman-Rakic, and X. J. Wang, Cereb. Cortex **10**, 910 (2000).
[10] E. Izhikevich, *Dynamical Systems in Neuroscience. The Geometry of Excitability and Bursting* (The MIT Press, Cambridge, MA, 2006).
[11] G. B. Ermentrout, Scholarpedia **3**, 1398 (2008).
[12] P. E. Latham, B. J. Richmond, P. G. Nelson, and S. Nirenberg, J. Neurophysiol. **83**, 808 (2000).
[13] D. Hansel and G. Mato, Neural Comput. **15**, 1 (2003).
[14] M. Dipoppa and B. S. Gutkin, Proc. Natl. Acad. Sci. U. S. A. **110**, 12828 (2013).
[15] N. Brunel and X. J. Wang, J. Comput. Neurosci. **11**, 63 (2001).
[16] X. J. Wang, Physiol. Rev. **90**, 1195 (2010).
[17] B. S. Gutkin, C. R. Laing, C. L. Colby, C. C. Chow, and G. B. Ermentrout, J. Comput. Neurosci. **11**, 121 (2001).
[18] X. J. Wang, J. Neurosci. **19**, 9587 (1999).
[19] P. Jedlicka, T. Deller, B. S. Gutkin, and K. H. Backus, Hippocampus **21**, 885 (2011).
[20] K. M. Stiefel, B. S. Gutkin, and T. J. Sejnowski, PLoS One **3**, e3947 (2008).
[21] Y. Tsuno, N. W. Schultheiss, and M. E. Hasselmo, J. Physiol. **591**, 2611 (2013).
[22] B. Gutkin, J. Jost, and H. C. Tuckwell, Theor. Biosci. **127**, 135 (2008).
[23] H. C. Tuckwell, J. Jost, and B. S. Gutkin, Phys. Rev. E **80**, 031907 (2009).